



HAL
open science

The transverse asymmetry $A_{T'}$ from quasi-elastic ${}^3\overline{\text{He}}(\vec{e}, e')$ process and the neutron magnetic form factor.

Wei-Jiang Xu, D. Dutta, F. Xiong, B. Anderson, L. Auerbach, T. Averett, W. Bertozzi, T. Black, J. Calarco, L. Cardman, et al.

► To cite this version:

Wei-Jiang Xu, D. Dutta, F. Xiong, B. Anderson, L. Auerbach, et al.. The transverse asymmetry $A_{T'}$ from quasi-elastic ${}^3\overline{\text{He}}(\vec{e}, e')$ process and the neutron magnetic form factor.. *Physical Review Letters*, 2000, 85, pp.2900-2904. <in2p3-00006274>

HAL Id: in2p3-00006274

<https://in2p3.hal.science/in2p3-00006274v1>

Submitted on 26 Sep 2000

HAL is a multi-disciplinary open access archive for the deposit and dissemination of scientific research documents, whether they are published or not. The documents may come from teaching and research institutions in France or abroad, or from public or private research centers.

L'archive ouverte pluridisciplinaire **HAL**, est destinée au dépôt et à la diffusion de documents scientifiques de niveau recherche, publiés ou non, émanant des établissements d'enseignement et de recherche français ou étrangers, des laboratoires publics ou privés.



HAL Authorization

The Transverse Asymmetry $A_{T'}$ from Quasi-elastic ${}^3\vec{\text{He}}(\vec{e}, e')$ Process and the Neutron Magnetic Form Factor

W. Xu,¹² D. Dutta,¹² F. Xiong,¹² B. Anderson,¹⁰ L. Auerbach,¹⁹ T. Averett,³ W. Bertozzi,¹² T. Black,¹² J. Calarco,²² L. Cardman,²⁰ G. D. Cates,¹⁵ Z. W. Chai,¹² J. P. Chen,²⁰ S. Choi,¹⁹ E. Chudakov,²⁰ S. Churchwell,⁴ G. S. Corrado,¹⁵ C. Crawford,¹² D. Dale,²¹ A. Deur,^{11,20} P. Djawotho,³ B. W. Filippone,¹ J. M. Finn,³ H. Gao,¹² R. Gilman,^{17,20} A. V. Glamazdin,⁹ C. Glashauser,¹⁷ W. Glöckle,¹⁶ J. Golak,⁸ J. Gomez,²⁰ V. G. Gorbenko,⁹ J.-O. Hansen,²⁰ F. W. Hersman,²² D. W. Higinbotham,²⁴ R. Holmes,¹⁸ C. R. Howell,⁴ E. Hughes,¹ B. Humensky,¹⁵ S. Incerti,¹⁹ C.W. de Jager,²⁰ J. S. Jensen,¹ X. Jiang,¹⁷ C. E. Jones,¹ M. Jones,³ R. Kahl,¹⁸ H. Kamada,¹⁶ A. Kievsky,⁵ I. Kominis,¹⁵ W. Korsch,²¹ K. Kramer,³ G. Kumbartzki,¹⁷ M. Kuss,²⁰ E. Lakurigi,¹⁹ M. Liang,²⁰ N. Liyanage,²⁰ J. LeRose,²⁰ S. Malov,¹⁷ D.J. Margaziotis,² J. W. Martin,¹² K. McCormick,¹² R. D. McKeown,¹ K. McIlhany,¹² Z.-E. Meziani,¹⁹ R. Michaels,²⁰ G. W. Miller,¹⁵ J. Mitchell,²⁰ S. Nanda,²⁰ E. Pace,^{7,23} T. Pavlin,¹ G. G. Petratos,¹⁰ R. I. Pomatsalyuk,⁹ D. Pripstein,¹ D. Prout,¹⁰ R. D. Ransome,¹⁷ Y. Roblin,¹¹ M. Rvachev,¹² A. Saha,²⁰ G. Salmè,⁶ M. Schnee,¹⁹ T. Shin,¹² K. Slifer,¹⁹ P. A. Souder,¹⁸ S. Strauch,¹⁷ R. Suleiman,¹⁰ M. Sutter,¹² B. Tipton,¹² L. Todor,¹⁴ M. Viviani,⁵ B. Vlahovic,^{13,20} J. Watson,¹⁰ C. F. Williamson,¹⁰ H. Witala,⁸ B. Wojtsekhowski,²⁰ J. Yeh,¹⁸ P. Żolnierczuk²¹

¹California Institute of Technology, Pasadena, CA 91125, USA

²California State University, Los Angeles, Los Angeles, CA 90032, USA

³College of William and Mary, Williamsburg, VA 23187, USA

⁴Duke University, Durham, NC 27708, USA

⁵INFN, Sezione di Pisa, Pisa, Italy

⁶INFN, Sezione di Roma, I-00185 Rome, Italy

⁷INFN, Sezione Tor Vergata, I-00133 Rome, Italy

⁸Institute of Physics, Jagellonian University, PL-30059 Cracow, Poland

⁹Kharkov Institute of Physics and Technology, Kharkov 310108, Ukraine

¹⁰Kent State University, Kent, OH 44242, USA

¹¹LPC, Université Blaise Pascal, F-63177 Aubière, France

¹²Massachusetts Institute of Technology, Cambridge, MA 02139, USA

¹³North Carolina Central University, Durham, NC 27707, USA

¹⁴Old Dominion University, Norfolk, VA 23508, USA

¹⁵Princeton University, Princeton, NJ 08544, USA

¹⁶Ruhr-Universität Bochum, D-44780 Bochum, Germany

¹⁷Rutgers University, Piscataway, NJ 08855, USA

¹⁸Syracuse University, Syracuse, NY 13244, USA

¹⁹Temple University, Philadelphia, PA 19122, USA

²⁰Thomas Jefferson National Accelerator Facility, Newport News, VA 23606, USA

²¹University of Kentucky, Lexington, KY 40506, USA

²²University of New Hampshire, Durham, NH 03824, USA

²³Dipartimento di Fisica, Università di Roma "Tor Vergata", Rome, Italy

²⁴University of Virginia, Charlottesville, VA 22903, USA

(26 July 2000)

We have measured the transverse asymmetry $A_{T'}$ in ${}^3\vec{\text{He}}(\vec{e}, e')$ quasi-elastic scattering in Hall A at Jefferson Lab with high statistical and systematic precision for Q^2 -values from 0.1 to 0.6 (GeV/c)². The neutron magnetic form factor G_M^n was extracted based on Faddeev calculations for $Q^2 = 0.1$ and 0.2 (GeV/c)² with an experimental uncertainty of less than 2%.

13.40.Fn, 24.70.+s, 25.10.+s, 25.30.Fj

The electromagnetic form factors of the nucleon have been a longstanding subject of interest in nuclear and particle physics. They describe the distribution of charge and magnetization within nucleons and allow sensitive

tests of nucleon models based on Quantum Chromodynamics. This advances our knowledge of nucleon structure and provides a basis for the understanding of more complex strongly interacting matter in terms of quark and gluon degrees of freedom.

The proton electromagnetic form factors have been determined with good precision at low values of the squared four-momentum transfer, Q^2 , using Rosenbluth separation of elastic electron-proton cross sections, and more recently at higher Q^2 using a polarization transfer technique [1]. The corresponding neutron form factors are known with much poorer precision because of the lack of free neutron targets. Over the past decade, with the advent of new experimental techniques such as polarized

beams and targets, the precise determination of both the neutron electric form factor, G_E^n , and the magnetic form factor, G_M^n , has therefore become a focus of experimental activity. Considerable attention has been devoted to the precise measurement of G_M^n . While knowledge of G_M^n is interesting in itself, it is also required for the determination of G_E^n , which is usually measured via the ratio G_E^n/G_M^n . Further, precise data for the nucleon electromagnetic form factors are essential for the analysis of parity violation experiments [2,3] designed to probe the strangeness content of the nucleon, where the quantities of interest appear in combination with the electromagnetic form factors.

Until recently, most data on G_M^n had been deduced from elastic and quasi-elastic electron-deuteron scattering. For inclusive measurements, this procedure requires the separation of the longitudinal and transverse cross sections and the subsequent subtraction of a large proton contribution. Thus, it suffers from large theoretical uncertainties due in part to the deuteron model employed and in part to corrections for final-state interactions (FSI) and meson-exchange currents (MEC). The proton subtraction can be avoided by measuring the neutron in coincidence ($d(e, e'n)$) [4], and the sensitivity to nuclear structure can be greatly reduced by taking the cross-section ratio of $d(e, e'n)$ to $d(e, e'p)$ at quasi-elastic kinematics. Several recent experiments [5–7] have employed the latter technique to extract G_M^n with uncertainties of $<2\%$ [7] for Q^2 -values from 0.1 to 0.8 (GeV/c)². While this precision is very good, there is considerable disagreement among the results [4–7] with respect to the absolute value of G_M^n . All these exclusive experiments require the absolute calibration of the neutron detection efficiency, which is difficult.

An alternative approach to a precision measurement of G_M^n is through the inclusive quasi-elastic reaction ${}^3\text{He}(\vec{e}, e')$. In comparison to deuterium experiments, this technique employs a different target and relies on polarization degrees of freedom. It is thus subject to completely different systematics. A pilot experiment using this technique was carried out at MIT-Bates and a result for G_M^n was extracted [8]. In this Letter, we report the first precision measurement of G_M^n using a polarized ${}^3\text{He}$ target.

Polarized ${}^3\text{He}$ is useful for studying the neutron electromagnetic form factors because of the unique spin structure of the ${}^3\text{He}$ ground state, which is dominated by a spatially symmetric S wave in which the proton spins cancel and the spin of the ${}^3\text{He}$ nucleus is carried by the unpaired neutron [9,10]. The spin-dependent contribution to the ${}^3\text{He}(\vec{e}, e')$ cross section is completely contained in two nuclear response functions, a transverse response $R_{T'}$ and a longitudinal-transverse response $R_{TL'}$. These appear in addition to the spin-independent longitudinal and transverse responses R_L and R_T . $R_{T'}$ and $R_{TL'}$ can

be isolated experimentally by forming the spin-dependent asymmetry A defined as $A = (\sigma^{h+} - \sigma^{h-})/(\sigma^{h+} + \sigma^{h-})$, where $\sigma^{h\pm}$ denotes the cross section for the two different helicities of the polarized electrons. In terms of the nuclear response functions, A can be written [11]

$$A = \frac{-(\cos\theta^* \nu_{T'} R_{T'} + 2 \sin\theta^* \cos\phi^* \nu_{TL'} R_{TL'})}{\nu_L R_L + \nu_T R_T} \quad (1)$$

where the ν_k are kinematic factors and θ^* and ϕ^* are the polar and azimuthal angles of target spin with respect to the 3-momentum transfer vector \mathbf{q} . The response functions R_k depend on Q^2 and the electron energy transfer ω . By choosing $\theta^* = 0$, *i.e.* by orienting the target spin parallel to the momentum transfer \mathbf{q} , one selects the transverse asymmetry $A_{T'}$ (proportional to $R_{T'}$).

Because the ${}^3\text{He}$ nuclear spin is carried mainly by the neutron, $R_{T'}$ at quasi-elastic kinematics contains a dominant neutron contribution and is essentially proportional to $(G_M^n)^2$, similar to elastic scattering from a free neutron. Unlike the free neutron case, however, the unpolarized part of the cross section (the denominator in Eq. (1)) contains contributions from both the protons and the neutron in the nucleus. Therefore, $A_{T'}$ is expected to first order to have the form $(G_M^n)^2/(a + b(G_M^n)^2)$ in the plane-wave impulse approximation (PWIA), where a is much larger than $b(G_M^n)^2$ at low Q^2 . While measurements of G_M^n using deuterium targets enhance the sensitivity to the neutron form factor by detecting the neutron in coincidence, a similar enhancement occurs in inclusive scattering from polarized ${}^3\text{He}$ because of the cancellation of the proton spins in the ground state. This picture has been confirmed by several PWIA calculations [12,13], as well as a more recent and more advanced calculation which fully includes FSI [14]. Thus, the inclusive asymmetry $A_{T'}$ in the vicinity of the ${}^3\text{He}$ quasi-elastic peak is most sensitive to the neutron magnetic form factor.

The experiment was carried out in Hall A at the Thomas Jefferson National Accelerator Facility (JLab), using a longitudinally polarized continuous wave electron beam of 10 μA current incident on a high-pressure polarized ${}^3\text{He}$ gas target [15]. The target was polarized by spin-exchange optical pumping at a density of 2.5×10^{20} nuclei/cm³ using rubidium as the spin-exchange medium. The beam and target polarizations were approximately 70% and 30%, respectively, and the beam helicity was flipped at a rate of 1 Hz (30 Hz for part of the experiment). To improve the optical pumping efficiency, the target contained a small admixture of nitrogen ($\sim 10^{18}$ cm⁻³). Backgrounds from the target cell walls and the nitrogen admixture were determined in calibration measurements using a reference cell with the same dimensions as those of the ${}^3\text{He}$ target cell. The background levels were a few percent of the full target yield. The background from rubidium was negligible.

Six kinematic points were measured corresponding to

$Q^2 = 0.1$ to 0.6 $(\text{GeV}/c)^2$ in steps of 0.1 $(\text{GeV}/c)^2$. An incident electron beam energy of 0.778 GeV was employed for the two lowest Q^2 values of the experiment and the remaining points were completed at an incident beam energy of 1.727 GeV. To maximize the sensitivity to $A_{T'}$, the target spin was oriented at 62.5° to the right of the incident electron momentum direction. This corresponds to θ^* from -8.5° to 6° , resulting in a contribution to the asymmetry due to $R_{TL'}$ of less than 2% at all kinematic settings, as determined from PWIA. To allow systematic checks, the target spin direction was rotated by 180° every 24-48 hours, and the overall sign of the beam helicity was periodically reversed at the polarized electron injector gun by inserting a $\lambda/2$ plate, resulting in four different combinations of beam and target polarization states.

Electrons scattered from the target were observed in the two Hall A High Resolution Spectrometers, HRSe and HRSh. Both spectrometers were configured to detect electrons in single-arm mode using nearly identical detector packages consisting of two dual-plane vertical drift chambers for tracking, two planes of segmented plastic scintillators for trigger formation, and a CO_2 gas Cherenkov detector and Pb-glass total-absorption shower counter for pion rejection. The spectrometer momentum and angular acceptances were approximately $\pm 4.5\%$ and 5.5 msr, respectively. The HRSe was set for quasi-elastic kinematics while the HRSh detected elastically scattered electrons. Since the elastic asymmetry can be calculated very well at low Q^2 using the well-known elastic form factors of ^3He [16], the elastic measurement allows precise monitoring of the product of the beam and target polarizations, $P_t P_b$. For the incident electron beam energy of 0.778 GeV, the HRSh was set to $Q^2 = 0.1$ for the elastic scattering kinematics and $P_t P_b$ can be determined to better than 2%. For the incident beam energy of 1.727 GeV, $P_t P_b$ can be determined to better than 3% at $Q^2 = 0.2$ $(\text{GeV}/c)^2$ for the elastic scattering. Standard Møller and NMR polarimetry were performed as a cross-check of the elastic polarimetry. The $P_t P_b$ averaged over all six quasi-elastic kinematic settings of this experiment determined from the elastic polarimetry was $0.208 \pm 0.001 \pm 0.005$, where the errors are statistical and systematic, respectively. Combining the Møller and the NMR measurement, the average $P_t P_b$ was 0.215 ± 0.013 with the error being the total systematic error.

The yield for each electron helicity state was corrected by its corresponding charge and computer deadtime, and the raw experimental asymmetry was extracted as a function of ω for all six kinematic settings. The raw asymmetry was then corrected for dilutions due to scattering from the empty target walls, the nitrogen content and $P_t P_b$. The physics asymmetry $A_{T'}$ was obtained after corrections for radiative effects. Continuum radiative corrections were calculated using the covariant formalism of Akushevich *et al.* [18], which was generalized to quasi-elastic kinematics. This procedure requires knowl-

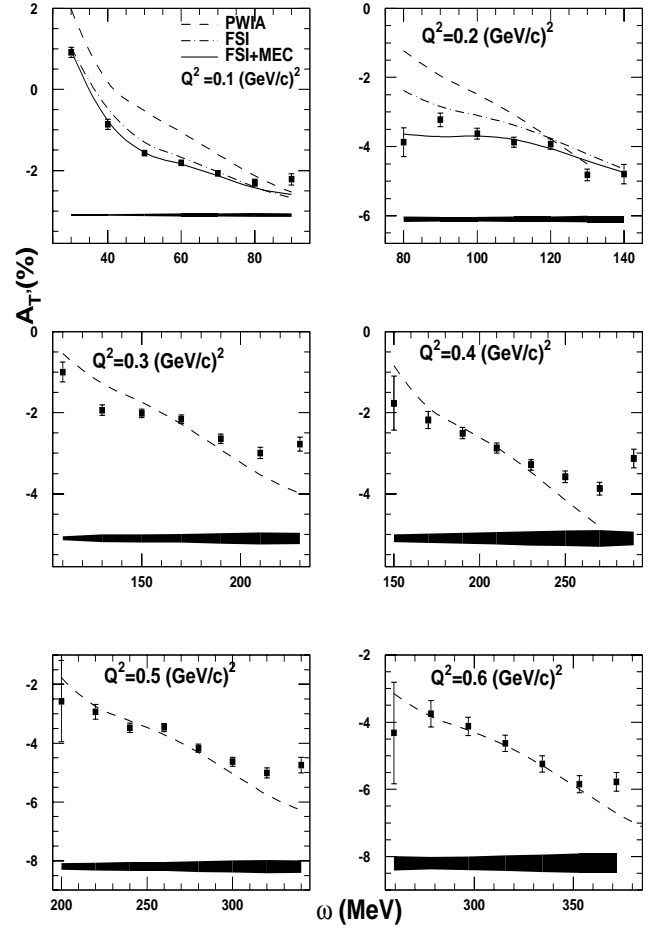


FIG. 1. The transverse asymmetry $A_{T'}$ at $Q^2=0.1-0.6$ $(\text{GeV}/c)^2$. The PWIA calculations are shown as dashed curves. The Faddeev calculations which include FSI only and FSI and MEC are shown as dash-dotted and solid curves, respectively.

edge of ^3He nuclear response functions at various kinematic points. These response functions were obtained from the full Faddeev calculation for $Q^2 = 0.1$ and 0.2 $(\text{GeV}/c)^2$ and the PWIA calculation [12] for $Q^2 = 0.3$ to 0.6 $(\text{GeV}/c)^2$.

Results for $A_{T'}$ as a function of ω are shown in Fig. 1 for all six kinematic settings of the experiment. The error bars on the data are statistical only, and the total experimental systematic error is indicated as an error band in each figure. PWIA calculations [12] using the AV18 for the NN interaction potential and the Höhler nucleon form factor parametrization [19] are shown as dashed lines. The Faddeev calculations with FSI only and with both FSI and MEC using the Bonn-B potential and the Höhler form factor parametrization are shown as dash-dotted lines and solid lines, respectively, for

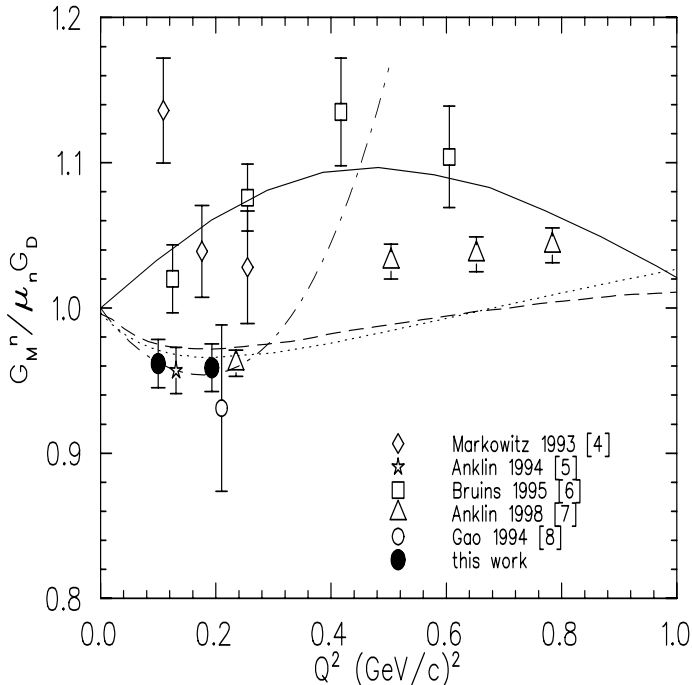


FIG. 2. The neutron magnetic form factor G_M^n in units of the standard dipole form factor $(1 + Q^2/0.71)^{-2}$, as a function of Q^2 , along with previous measurements and theoretical models. The Q^2 points of Anklin 94 [5] and Gao 94 [8] have been shifted slightly for clarity. The solid curve is a recent cloudy bag model calculation [23], the long dashed curve is a recent calculation based on a fit of the proton data using dispersion theoretical arguments [24], and the dotted curve is from the Höhler [19] parametrization. The dash-dotted curve is an analysis based on the relativistic baryon chiral perturbation theory [25].

$Q^2 = 0.1$ and 0.2 (GeV/c) 2 . All theory results were averaged over the spectrometer acceptances using a Monte Carlo simulation. The systematic uncertainty in $A_{T'}$ includes contributions from $P_t P_b$, background subtraction, radiative corrections, helicity-correlated false asymmetries, and pion contamination. A Monte Carlo simulation code was employed to determine $P_t P_b$ from the measured elastic asymmetry, taking into account the spectrometer acceptance, energy loss, detector resolutions, and radiative effects. The total uncertainty in determining $P_t P_b$ is dominated by the uncertainties in the ^3He elastic form factors. The overall systematic uncertainty of $A_{T'}$ is 2% for Q^2 values of 0.1 and 0.2 (GeV/c) 2 dominated by the uncertainty in determining $P_t P_b$, and 5% for Q^2 values of 0.3 to 0.6 (GeV/c) 2 dominated by the uncertainty in the radiative correction, which can be reduced with improved theoretical calculations for these values of Q^2 .

The state-of-the-art three-body calculation treats the ^3He target state and the 3N scattering states in the nuclear matrix element in a consistent way by solving the corresponding 3N Faddeev equations [20]. The MEC effects were calculated using the prescription of Riska [21], which includes π - and ρ -like exchange terms. While the

agreement between the data and full calculations is very good at $Q^2 = 0.1$ and 0.2 (GeV/c) 2 , the full calculation is not expected to be applicable at higher Q^2 because of its fully non-relativistic framework. A full calculation within the framework of relativity is highly desirable.

To extract G_M^n for the two lowest Q^2 kinematics, the transverse asymmetry data were averaged over a 30 MeV bin around the quasi-elastic peak. The full Faddeev calculation including MEC [22] was employed to generate $A_{T'}$ as a function of G_M^n in the same ω region. By comparing the measured asymmetries with the predictions, the G_M^n values at $Q^2 = 0.1$ and 0.2 (GeV/c) 2 were extracted. The extracted values of G_M^n are shown in Fig. 2 along with results from previous measurements and several theoretical calculations. The uncertainties shown are the quadrature sum of the statistical and experimental systematic uncertainties. These results are tabulated in Table I.

Since the full calculation described above is at present the only theoretical calculation available which treats FSI and MEC under the present experimental conditions, it is important to mention one highly nontrivial internal test. The nuclear response functions for the inclusive scattering on ^3He were calculated in two independent ways by either integrating explicitly over the pd and ppn breakup channels (with full inclusion of FSI) or using a completeness relation [26]. The agreement between these two approaches is within 1% [27]. The Faddeev based formalism has been applied to other reaction channels and good agreements have been found with experimental results [27], in particular the most recent NIKHEF data on A_y^0 at $Q^2 = 0.16$ (GeV/c) 2 from the quasielastic $^3\text{He}(\bar{e}, e'n)$ process [28].

To investigate the theoretical uncertainty in extracting G_M^n at $Q^2 = 0.1$ and 0.2 (GeV/c) 2 , the full calculations were carried through with two different NN potentials, Bonn-B and AV18. The difference in the calculated asymmetries is less than 1% around the quasi-elastic peak. The uncertainty due to G_E^p , G_M^p , and G_E^n was studied by varying these quantities over their experimental errors, and the range of variation in the calculated asymmetry was 1%. The uncertainty due to MEC was estimated by comparing results with and without the inclusion of the Δ isobar current. At $Q^2 = 0.1$ and 0.2 (GeV/c) 2 relativistic corrections to $A_{T'}$ were estimated to be 2% and 4% [29] around the quasi-elastic peak, respectively. Based on these studies, the overall theoretical uncertainty in calculating $A_{T'}$ was estimated to be 3.8% and 5.1% for $Q^2 = 0.1$ and 0.2 (GeV/c) 2 , respectively. This results in an estimated theoretical uncertainty of 1.9% and 2.6% in extracting G_M^n for these two Q^2 points correspondingly, which can be reduced once relativistic full calculations become available. The errors on G_M^n from present work shown in Fig. 2 and Table I are experimental errors only, which do not include the theoretical

| Q^2 (GeV/c) ² | $G_M^n/G_M^n(\text{Dipole})$ | Uncertainties |
|----------------------------|------------------------------|-----------------------|
| 0.1 | 0.962 | $\pm 0.014 \pm 0.010$ |
| 0.2 | 0.959 | $\pm 0.013 \pm 0.010$ |

TABLE I. G_M^n as a function of Q^2 , the uncertainties are statistical and experimental systematic, respectively.

uncertainties discussed above.

In conclusion the inclusive transverse asymmetry A_{TV} from the quasi-elastic ${}^3\text{He}(\vec{e}, e')$ process has been measured with high precision at Q^2 -values from 0.1 to 0.6 (GeV/c)². Using a full Faddeev calculation which includes FSI and MEC we have extracted the neutron magnetic form factor G_M^n at Q^2 values of 0.1 and 0.2 (GeV/c)². The extracted values of G_M^n at Q^2 of 0.1 and 0.2 (GeV/c)² agree with the previous measurements of Anklin *et al.* [5,7]. The present experiment provides the first precision data on G_M^n using a fundamentally different experimental approach than previous experiments. Thus it is a significant step towards understanding the discrepancy among the existing data sets in the low- Q^2 region. Although we have presented precise data on A_{TV} at higher Q^2 (0.3 - 0.6 (GeV/c)²) in this Letter, full calculations are at present not available for these values of Q^2 to allow the extraction of G_M^n with high precision. Theoretical efforts are currently underway to extend the full calculation to higher Q^2 [30].

We thank the Hall A technical staff and the Jefferson Lab Accelerator Division for their outstanding support during this experiment. We also thank S. Ishikawa for providing us with his calculations in the early stage of this work, T. W. Donnelly for helpful discussions, and O.N. Ozkul for the target polarization analysis. This work was supported in part by the U. S. Department of Energy, DOE/EPSCoR, the U. S. National Science Foundation, the Science and Technology Cooperation Germany-Poland and the Polish Committee for Scientific Research, the Ministero dell'Università e della Ricerca Scientifica e Tecnologica (Murst), the French Commissariat à l'Énergie Atomique, Centre National de la Recherche Scientifique (CNRS) and the Italian Istituto Nazionale di Fisica Nucleare (INFN). This work was supported by DOE contract DE-AC05-84ER40150 under which the Southeastern Universities Research Association (SURA) operates the Thomas Jefferson National Accelerator Facility. The numerical calculations were performed on the PVP machines at the U. S. National Energy Research Scientific Computer Center (NERSC) and the CRAY T90 of the NIC in Jülich.

- [2] B. Mueller *et al.*, Phys. Rev. Lett. **78**, 3824 (1997).
[3] K.A. Aniol *et al.*, Phys. Rev. Lett. **82**, 1096 (1999).
[4] P. Markowitz *et al.*, Phys. Rev. C **48**, R5 (1993).
[5] H. Anklin *et al.*, Phys. Lett. **B336**, 313 (1994).
[6] E.E.W. Bruins *et al.*, Phys. Rev. Lett. **75**, 21 (1995).
[7] H. Anklin *et al.*, Phys. Lett. **B428**, 248 (1998).
[8] H. Gao *et al.*, Phys. Rev. C **50**, R546 (1994); H. Gao, Nucl. Phys. **A631**, 170c (1998).
[9] B. Blankleider and R.M. Woloshyn, Phys. Rev. C **29**, 538 (1984).
[10] J.L. Friar *et al.*, Phys. Rev. C **42**, 2310 (1990).
[11] T.W. Donnelly and A.S. Raskin, Ann. Phys. **169**, 247 (1986).
[12] A. Kievsky, E. Pace, G. Salmè, M. Viviani, Phys. Rev. C **56**, 64 (1997).
[13] R.-W. Schulze and P. U. Sauer, Phys. Rev. C **48**, 38 (1993).
[14] S. Ishikawa *et al.*, Phys. Rev. C **57**, 39 (1998).
[15] J.S. Jensen, Ph.D. Thesis, California Institute of Technology, 2000 (unpublished); P.L. Anthony *et al.*, Phys. Rev. D, **54** 6620 (1996); http://www.jlab.org/e94010/tech_notes.html.
[16] A. Amroun *et al.*, Nucl. Phys. **A579**, 596 (1994); C.R. Otterman *et al.*, Nucl. Phys. **A435**, 688 (1985); P.C. Dunn *et al.*, Phys. Rev. C **27**, 71 (1983).
[17] O.N. Ozkul, Senior Thesis, MIT (2000), unpublished.
[18] I.V. Akushevich and N.M. Shumeiko, J. Phys. G **20**, 513 (1994); F. Xiong *et al.*, in preparation for publication.
[19] G. Höhler *et al.*, Nucl. Phys. **B114**, 505 (1976).
[20] J. Golak *et al.*, Phys. Rev. C **51**, 1638 (1995).
[21] D.O. Riska, Phys. Scr. **31**, 471 (1985).
[22] V.V. Kotlyer, H. Kamada, W. Glöckle, J. Golak, Few-Body Syst. **28**, 35 (2000).
[23] D.H. Lu, A.W. Thomas, A.G. Williams, Phys. Rev. C **57**, 2628 (1998).
[24] P. Mergell, U.-G. Meißner, D. Drechsel, Nucl. Phys. **A596**, 367 (1996).
[25] B. Kubis, U.-G. Meißner, hep-ph/0007056.
[26] S. Ishikawa *et al.*, Phys. Lett. **B339**, 293 (1994).
[27] J. Golak *et al.*, Phys. Rev. C **52**, 1216 (1995); C.M. Spaltro *et al.*, Phys. Rev. Lett. **81**, 2870 (1998); W. Glöckle *et al.*, Electronuclear Physics with Internal Targets and the Blast Detector, edited by R. Alarcon and R.G. Milner, 185 (1999).
[28] H.R. Poolman, Ph.D. Thesis, Vrije Universiteit Amsterdam (1999).
[29] T.W. Donnelly, private communication.
[30] W. Glöckle, private communication.

[1] M. Jones *et al.*, Phys. Rev. Lett. **84**, 1398 (2000).